Improved Moth-Flame Optimization for Optimal Reactive Power Dispatch in Large-Scale Systems

Lam Buu Qui[1] anh Khai Phuc Nguyen[1,2,*]

ARTICLEINFO

Article history:
Received: 15 October 2020
Revised: 17 November 2020
Accepted: 23 November 2020

Keywords:
Improved Moth-flame optimization
Reactive power dispatch
Large-scale systems

ABSTRACT

This paper presents an Improved Moth-flame Optimization to minimize power loss in the grids considering the constraints on the operation of equipment in the power system as well as the capacity of the transmission line. In this improvement, the number of flames is reduced exponentially, resulting in better convergence problems, especially in large scale problems. For problems in general and technical problems in particular, the first criteria should be considered as the best value and the average value of the solution. The proposed method has well addressed the requirements and has increased the accuracy and reliability of the MFO method. The IEEE power systems have been obtained to show that the performance of the proposed Improved Moth-flame Optimization is better than the one of the conventional method.

1. INTRODUCTION

Since 2015, Seyedali Mirjalili has developed a powerful nature-inspired optimization entitled Moth-flame optimization (MFO) [16]. The method depends on the strategy of moths to identify their navigation in night. A moth is an insert in nature and usually earns food in night. The moth maintains a fixed angle with the moon to circle in night. Nonetheless, if the moths were attracted to artificial light sources, such as circle lights, it would be stuck in a deadly spiral fly path. Moth-flame optimization illustrates the spiral fly path of moths while searching the global optimum. Following works of Seyedali Mirjalili show that MFO is better than six well-known optimization techniques on seven basic tested benchmarks. The author applied the MFO for designing gear trains in mechanical engineering or three-bar truss in civil engineering. After Seyedali's works, Zhiming Li *et al.* proposed a combination of MFO and Levy flight for engineering design problems, also known as LMFO algorithm, Lévy-flight can prevent local convergence by diversifying the population of the problem, and this can make LMFO find an efficient optimal solution and more accurate results than the MFO algorithm [14]. On another hand, M. A. E. Aziz *et al.* made an observation of the MFO and Whale Optimization Algorithm for multilevel thresholding image segmentation. Five compared algorithms have been observed using a lot of standard photos. According to the conclusion, the MFO showed better results than the Whale Optimization Algorithm and the other swarm algorithms [9]. In addition, B. S. Yildiz and A. R. Yildiz employed the MFO to solve optimal setting parameters in manufacturing processes. The analytical results highlighted the effectiveness of the MFO in the optimization of manufacturing problems. The major purpose of the paper is to maximize the benefit for multi-tool milling service and handle many challenging constraints. The research indicates that the conventional MFO is powerful for problems on manufacturing optimization [28]. Therefore, MFO is also favorable to solve design engineering and multi-constraint multi-objective problems.

Optimal reactive power dispatch, shortly ORPD, is an optimal power distribution problem used in power systems. In which the elements that can control reactive power and regulate voltage include: generator output voltage, under-load voltage regulator of transformer (OLTC), reactive power sources such as capacitors or synchronous compensator will be adjusted for the main purpose of reducing power loss, strengthen the voltage profile or improving the security voltage index. The above problem is also studied and applied optimization methods to meet the multi-objective problem for a long time. Previously, some conventional approaches such as quadratic programming [18], Lagrange function [6] and linear programming [3] were applied. Nonetheless, the classical algorithms are only suitable for finding optimal solutions to scaled-down dilemmas. For large-scale obstacles, the calculation becomes more complicated and it is accessible to initiate the local optima. Nowadays metaheuristic techniques have been developed and prevailed. For instance, El Ela et al. employed an version of Differential

[1]*Ho Chi Minh University of Technology, 268 Ly Thuong Kiet Street, District 10, Ho Chi Minh City, Vietnam.*
[2]*Vietnam National University Ho Chi Minh City, Linh Trung Ward, Thu Duc District.*
**Corresponding author:* K. P. Nguyen; E-mail: phuckhai@hcmut.edu.vn.

evolution (DE) for solving ORPD [1]; S. Durairaj et al. proposed a version of Genetic algorithm (GA) for ORPD considering voltage stability enhancement [8]. Their works show that these evolutionary methods have been successful to search the global optima; however, each stochastic search method only effects on some problems. Hence, the development of these methods to find an effective algorithm is continued.

According to the original MFO, the new positions of moths are generated from the flames locating in the seeking space. The number of the flames is decreased by iterations. In this paper, the authors introduce a novel approach to enhance the original MFO to explore faster the optimal solution. The proposed strategy tries to reduce the number of flames by an exponential function. The proposed Improved Moth-Flame Optimization has been surveyed on 19 mathematical benchmarks and minimizes the power loss in the power system to compare the effectiveness with the original MFO.

This paper consists of seven parts. In the second part, we go into the details of the algorithm, the steps to implement the algorithm and the related formulas. The third part describes the improvement of the Moth-flame Optimization method. The fourth part will show the efficiency of the improved MFO algorithm compared to conventional MFO algorithm and other optimization methods through basic functions. The next part will introduce the ORPD problem, related constraints, fitness function and flowchart. The fifth part shows the analytical results. The conclusion and our future work are given in the final part.

2. MOTH-FLAME OPTIMIZATION ALGORITHM

Moth-flame Optimization is an optimization method inspired by moths when they move in a straight line over a great distance, this mechanism is called horizontal orientation. Moths will fly and keep a stable angle to the moon. For the reason that the moon is long-distance from the earth, they will always move in a straight line. However, they are easily trapped by artificial light sources and move in a spiral until they reach the light source as Fig. 1.

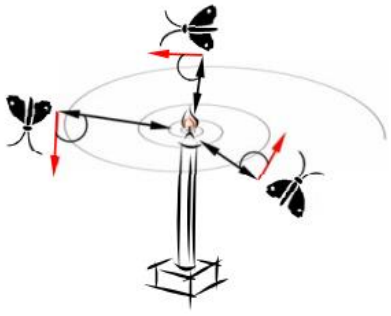

Fig. 1: Moths are trapped by flames

Basing on the fact that the path of the moth will converge when moving towards the artificial light source, the Moth-flame Optimization method has been introduced by Seyedali Mirjalili. Each moth in the MFO method represents a solution, if the number of populations is larger, the solution set will be diverse and our task is to find the location of the night butterfly. The flame, or artificial light source, preserves the moth's best position after each iteration. The position of the moth complying with the flame by the distance D_i is continuously updated in space in a spiral and is described by the equation.

$$S(M_i, F_j) = D_i \exp(bt)\cos(2\pi t) + F_j \quad (1)$$

The parameter t is randomly in the range [-1, 1], which supports to indicate how much the moth move close to the flame in the next iteration (t = 1 shows the farthest position to the flame, and t = -1 is the closest). Consequently, a hyper ellipse is gathered around the flame in all directions and the next position of the moth would be within the space. Figure 2 illustrates the shape of the logarithmic spiral which is defined by the constant b, and the position considering different t.

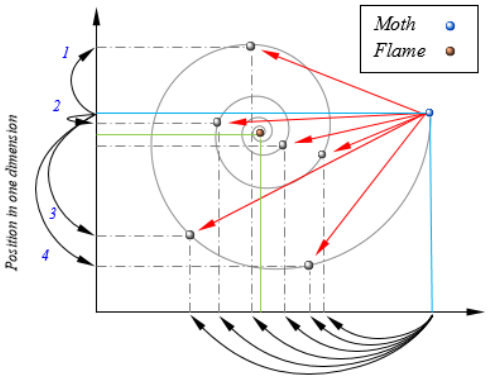

Fig. 2: Logarithmic spiral, seeking zone around a flame, and the moths with respect to *t*.

The distance D_i is based on the position of the moth M_i and the position of the flame F_j as follows:

$$D_i = \left|F_j - M_i\right| \quad (2)$$

We observe in Figure 3 the discovery and exploitation of moths in the one-dimensional search space. Searching takes place when the position of the moth follows the arrows labeled 1, 3 and 4. Exploration takes place when the position of the moth follows the arrow labeled 2. Several points can be drawn. out of this model as follow:

- On changing the value of t, a moth concentrates to any point in the vicinity of the flame.
- The lower t, the distance from the moth to the flame decreases.
- When the moth position gets closer to the fire, the number of location updates is increased.

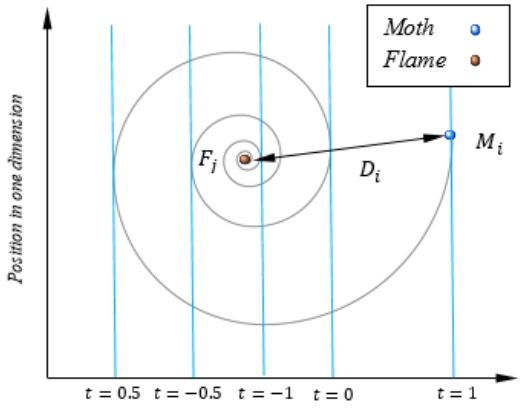

Fig. 3: The trajectory of the position of the moth concerning the flame in logarithm

The updated position of moths for *n* different locations in the search space downgrades the exploitation of the best promising solutions. To resolve this problem, Seyedali Mirjalili proposed a flexible mechanism for the number of flames *NF*.

$$NF = round\left(N - l * \frac{N-1}{T}\right) \quad (3)$$

where, *l*, *N*, and *T* indicate the instant number of iterations, the total of flames, and the total of iterations, respectively.

3. PROPOSED IMPROVED MOTH-FLAME OPTIMIZATION

We have seen the benefits of reducing the number of flames through each loop. It has had an effect in balancing the search and exploitation. However, in some large-scale problem, finding too much can make the problem easy to fall into the non-convergence case.

In this paper, the authors propose a solution to help moths find more effective in the space of search and exploitation of optimal solutions. Therefore, instead of the number of flames decreased after each loop follows a linear function. A proposed exponential function focuses and exploits the optimal results at the end of the algorithm. This is expected to bring more optimal results to the problem, especially in complex problems.

The formula of the proposed exponential function is the following:

$$NF = round\left(N^{\frac{-l}{T}+1}\right) \quad (4)$$

Figure 4 shows the converged strategy of the proposed improved and the conventional MFO.

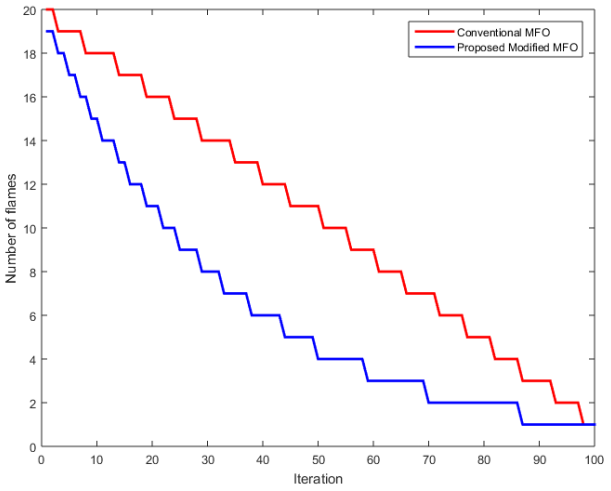

Figure 4: Number of flames after loops

4. THE EFFECTIVENESS OF IMPROVED MOTH-FLAME OPTIMIZATION IN PRACTICE

To validate the efficiency of the improved MFO algorithm over the traditional MFO algorithm and others, we evaluate the performance of the algorithms on a set of well-known mathematical functions. We employ 19 standard functions in the literature as testbeds for comparison ([19], 49-51). For more efficient testing, we divide the functions into three groups: unimodal, multi-modal, and composite. The unimodal functions (F1-F7) are used to evaluate the optimal exploitation of the algorithm because we do not have a local optimal. In contrast, multi-modal functions (F8-F13) can be used for local checking and are very useful for finding global solutions, avoiding algorithms falling into local solutions. Finally, the composite functions (F14-F19) are a combination of various rotation, displacement, and deflection multimodal test functions. It is a search space that is close to real problems, helping algorithms to prove their effectiveness in balancing discovery and exploiting the optimal solutions.

The details of the mathematical formulas of the test functions for the algorithms are presented in [16]. Because the conventional version of the uni-modal and multi-modal test functions are too elementary, Seyedali Mirjalili rotated the test functions using the rotation matrix proposed by Lorio and Li [12] and shift their optima at every run to enhance the complication of these functions.

Random optimization techniques require a minimum of 10 runs for the results to be statistically significant. Table A.1, Table A.2 and Table A.3 in the Appendix are the results of the algorithms after running 100 tests, which is enough for comparison between algorithms. The improved MFO algorithm will be compared with the latest variations of other stochastic algorithms to demonstrate its superiority: PSO [23], GSA, FPA [27], SMS [5], FA [26], and GA [11]. Figure 5, Figure 6 and Figure 7 compare the convergence profiles for Function F1 in the unimodal

function group, Function F8 in the multimodal function group and Function F15 in the composite function group of the proposed Improve MFO and the conventional MFO. Two methods are similar at the first stage of the searching process. However, at the end, the proposed method converses faster and reaches the optimal solution.

Most of the results from the test function show that the Improved MFO method is better than the conventional MFO method in particular and other methods in general. From here we will consider the actual problem as the Optimal Reactive Power Dispatch (ORPD) problem.

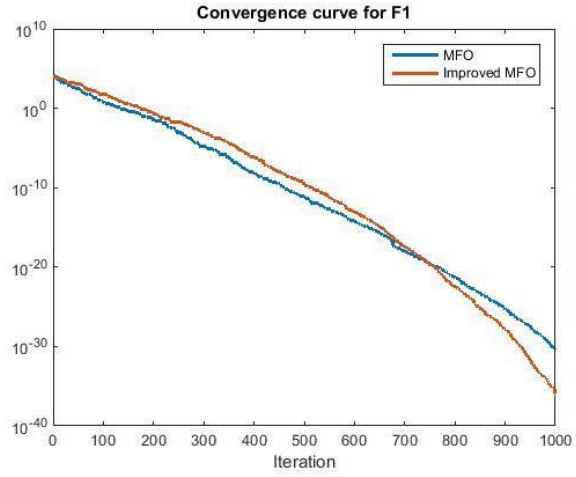

Fig. 5: Comparison about convergences profiles for Function F1 of proposed method.

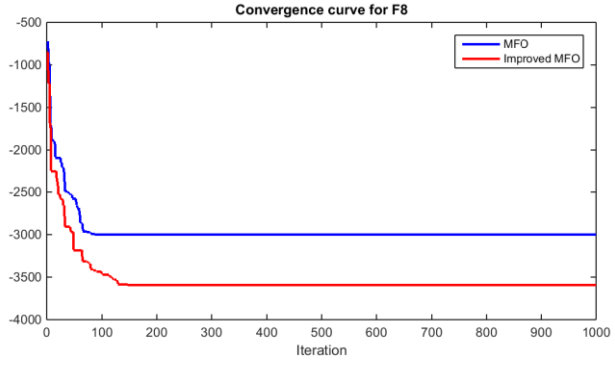

Fig. 6: Comparison about convergences profiles for Function F8 of proposed method.

5. OPTIMAL REACTIVE POWER DISPATCH

5.1 Objective function

The goal of the ORPD problem is to reduce power loss on the grid and maintain voltage quality. To achieve these goals, the most important issue is the control of reactive power sources such as: generator output voltage, under-load voltage regulator of transformer (OLTC), reactive power sources, etc. This is a typical and popular problem for power system operators, solving this problem has great significance.

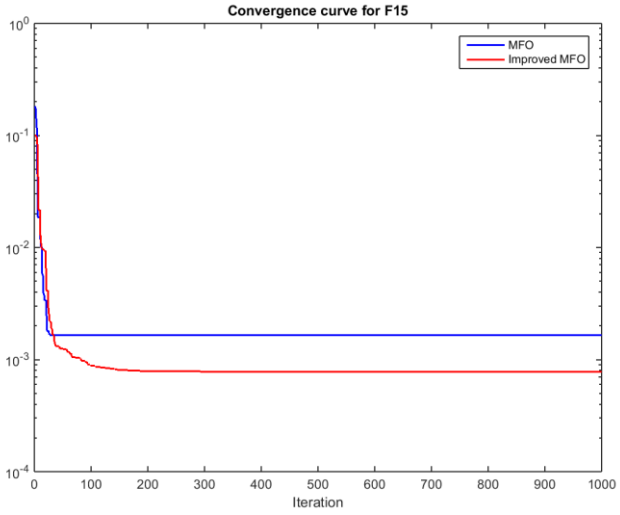

Fig. 7: Comparison about convergences profiles for Function F15 of proposed method.

The total active power loss P_{loss} is calculated from the current through line I_l and the resistance of the line R_l as follows:

$$P_{loss} = \sum_{l=1}^{br} R_l I_l^2 \tag{5}$$

5.2 IEEE 118-bus system

In this benchmark, we define optimal solutions in which they must satisfy all operating constraints such as power balance constraints, bus voltage limitations and transmission line capacity.

5.2.1 Power balance constraints

The solution of the ORPD problem satisfies the power balance condition, in which the transmit power and demand power must be balanced at each node. The above binding condition is expressed through the equation of active power and reactive power:

$$\begin{aligned} &P_{G,i} - P_{D,i} = \\ &= V_i \sum_{i=1}^{b} \left[V_j \left[G_{ij} \cos\left(\delta_i - \delta_j\right) + B_{ij} \sin\left(\delta_i - \delta_j\right) \right] \right] \end{aligned} \tag{6}$$

$$\begin{aligned} &Q_{G,i} - Q_{D,i} = \\ &= V_i \sum_{i=1}^{b} \left[V_j \left[G_{ij} \sin\left(\delta_i - \delta_j\right) - B_{ij} \sin\left(\delta_i - \delta_j\right) \right] \right] \end{aligned} \tag{7}$$

where,

- $P_{G,i}$ and $P_{D,i}$: the active generating power and demand power at the *i*-th bus, respectively;
- $Q_{G,i}$ and $Q_{D,i}$: the reactive of generating power and demand powers at the *i*-th bus, respectively.
- G_{ij} and B_{ij} : the real and imaginary components of element Y_{ij} of the admittance matrix, respectively.

5.2.2 Constraints of generators

The generator output voltage and power must be within the allowable limits as follows:

$$V_{i,\min}^{G} \le V_i^{G} \le V_{i,\max}^{G} \quad (8)$$

$$Q_{i,\min}^{G} \le Q_i^{G} \le Q_{i,\max}^{G} \quad (9)$$

5.2.3 Constraints of VAR controlled components:

The limited power of reactive power sources can be expressed as follows:

$$Q_{i,\min}^{C} \le Q_i^{C} \le Q_{i,\max}^{C} \quad (10)$$

The number of steps of a transformer is in a range follows:

$$T_{i,\min} \le T_i \le T_{i,\max} \quad (11)$$

5.2.4 Constraints of limited load bus voltages

The voltage on the bus bars must be handled in an allowable range to provide the power quality for the entire power system:

$$V_{i,\min}^{L} \le V_i^{L} \le V_{i,\max}^{L} \quad (12)$$

5.2.5 Limitation of transmission lines

The transmission capacity on the line must ensure the power conditions to avoid heat generation and faults on the power grid:

$$\left|S_{li}\right| \le S_{li}^{max} \quad (13)$$

5.3 Implementation of Moth-flame Optimization for ORPD

5.3.1 Solution vector

The problem mainly revolves around controllable variables such as the value of the generator's voltage V_{gn}, the compensation power of capacitor banks Q_{cn} or the voltage of the transformers with tap changer T_n and the dependent variables are the voltages of the load nodes V_{ln}, the apparent power transmitted on the line S_n and reactive power outputs of the generators Q_{gn}. The vector of controllable and dependent variable are as follows:

$$x = \left[V_{g1},...,V_{gn},Q_{C1},...,Q_{Cn},T_1,...,T_n\right] \quad (14)$$

$$u = \left[Q_{g1},...,Q_{gn},V_{l1},...,V_{ln},S_1,...,S_n\right] \quad (15)$$

5.3.2 Initialize initial value

We will use the boundary limits of the variables along with using the random distribution function *rand*() to initialize the first solution to the problem.

The larger the number of N solutions, the wider the search scope can help the problem converge with better results.

$$Solution = UpB + rand()(UpB - LowB) \quad (16)$$

where, *UpB* is the upper bound condition, *LowB* is the lower bound condition, *rand*() will return the random value of the uniform distribution function

5.3.3 Modeling constraints in the optimization function

• During the optimization process, all bound conditions must be handled simultaneously.

• The condition of active and reactive power balance can be completely satisfied by the power balancing algorithm because if this condition is not guaranteed, the problem will not converge and have no optimal results.

• The generator voltage, capacitor capacity and step settings of the multi-step transformer are controllable variables. Because of these constraints, they will automatically adjust themselves to the boundary limits when a new solution is created.

• The binding conditions of the dependent variables will be controlled by converting to an element in the optimal objective function.

• The fitness function is the combination of the objective function and the constraints of dependent variables through a penalty coefficient of *Kp*.

• For the constraints of the dependent variables, we use some limit functions such as $V^{lim}(x)$.

• In all cases used for testing, we use the penalty factor of 10^6. The fitness function is presented as follows:

$$FF = P_{loss} + \sum_{i=1}^{N_g}\left[Q_{Gi} - V_i^{\lim}\left(Q_{Gi}\right)\right]^2 + K_P\sum_{i=1}^{b}\left[V_i - V_i^{\lim}\left(V_i\right)\right]^2 + K_P\sum_{i=1}^{br}\left(\left|S_{li}\right| - S_{li}^{\max}\right)^2 \quad (17)$$

$$V^{\lim}(x) = \begin{cases} x_{\max}, \text{if} x > x_{\max} \\ x, \text{if} x_{\min} \le x \le x_{\max} \\ x_{\min}, \text{if} x < x_{\min} \end{cases} \quad (16)$$

5.4 Flowchart

The overall procedure of the proposed Improved Moth-flame Optimization for the Optimal Reactive Power Dispatch is given in Figure 8.

6. NUMERICAL RESULTS

The Moth-Flame Optimization has been evaluated to clarify the optimal problems of ORPD in four standard grid models of IEEE. In which, the calculation of power distribution is made by the Newton-Raphson method supported by the Matpower toolbox [29]. All case studies have been run on the personal computer with the Intel Corei7 1065G7 processor and 8Gb RAM.

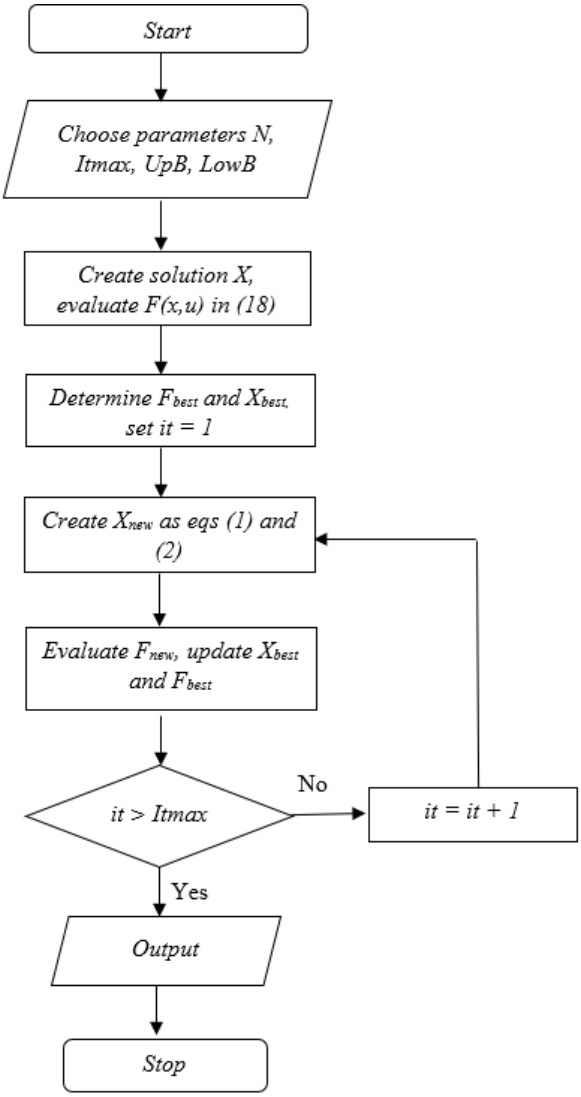

Fig. 8: Overall Procedure

6.1 Case study 1

The first study is the standard IEEE 30-bus system [2] including 06 generators, 24 load buses, and 41 branches. We plan to install nine reactive power sources on the tested system. In lines (6, 9), (6, 10), (4, 12), and (27, 28), there are four transformers with tap changers in each line. The limit of reactive power generation is given in [15] and the limit of the power flows of transmitted lines is given in [4]. We have to keep the generator voltage, transformer lap changers, and voltages at load buses in good condition as follows:

$$0.95 \le V_{gi} \le 1.1 \quad (19)$$

$$0.90 \le T_i \le 1.1 \quad (20)$$

$$0.95 \le V_{li} \le 1.1 \quad (21)$$

The value of the fitness function is given in Tab. 1. The result shows that the performance of the proposed Improved MFO is better than the conventional method. The best solution solved by the Improved MFO is slightly better, while the mean value and the standard deviation are smaller than the conventional MFO. The proposed IMFO has been compared with various versions of Grey Wolf Optimizer [25] and the Particle Swarm Optimization [13]. The result of IMFO is slightly better than the PSO-TVIW and other methods in the literature.

The load voltage profile of the proposed solution given by the Improved MFO is shown in Fig. 9. The initial off-limits voltage has disappeared and the load voltage is kept stable in the allowable region. The convergence results of the two methods are presented in Fig. 10 and Fig. 11.

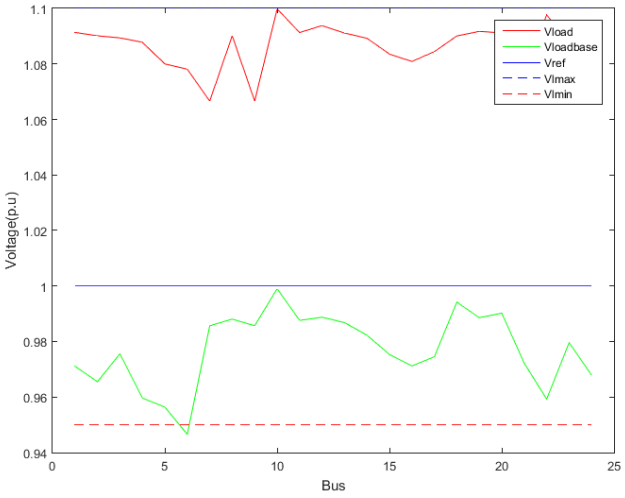

Fig. 9: Load voltage profile of IEEE 30-bus system when using Improved MFO Method.

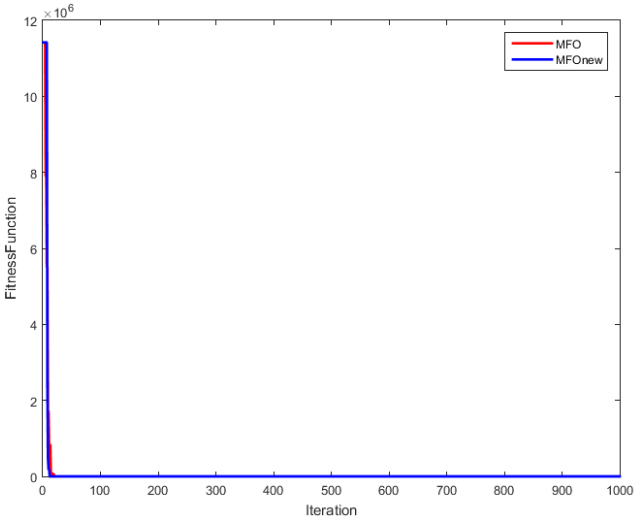

Fig. 10: Convergence characteristics of the compared methods

Table 1: Analytical results of conventional MFO and Improved MFO for the IEEE 30-bus system

Method	Best	Mean	SD
PSO-TVIW [13]	4.5129	4.5742	0.1907
PSO-TVAC [13]	4.5356	4.5912	0.0592
HPSO-TVAC [13]	4.5283	4.5581	0.0188
GWO [25]	4.5984	-	-
MFO	4.5128	4.5529	0.0962
IMFO	4.5128	4.55	0.0616

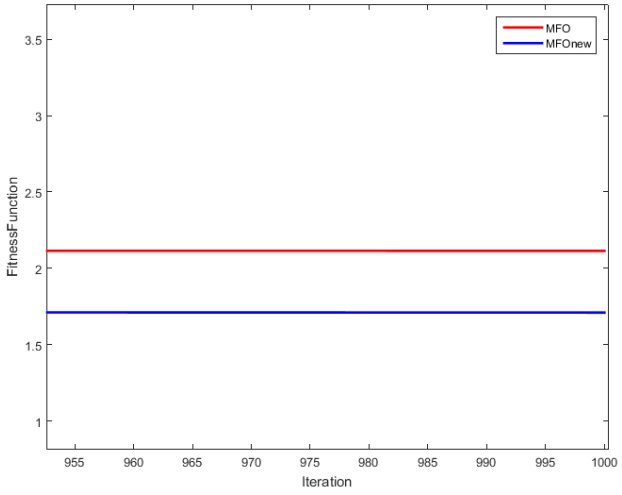

Fig. 11: Zoomed image of convergences at the end of search process

6.2 Case study 2

The second benchmark is the standard IEEE 57-bus system, a larger scale system. The tested one consists of 7 generators, 53 transmission lines, 57 load buses, and 17 transformers with online tap changers. We install three shunt reactive power sources at buses 18, 25, and 53. The constraints of all variables are taken from [10].

The analytical results two methods are presented in Tab. 2. All parameters of the Improved MFO method are clearly superior to the conventional MFO Method. In this case, the Firefly Algorithm (FA) gave better solution, while the IMFO is better than other methods such as: Differential Evolution (DE) and Grey Wolf Optimizer. Load voltage profile of the proposed methods is shown in Fig. 12. The optimal solution clearly satisfies all voltage constraints. The convergence results of the two methods are presented in Fig. 13 and Fig. 14.

Table 2: Analytical results of MFO and Improved MFO for the IEEE 57-bus system

Method	Best	Mean	SD
DE [17]	25.9556	-	-
FA [24]	24.4587	-	-
GWO [24]	24.7523	-	-
MFO	24.6702	25.0846	0.2075
IMFO	24.6202	25.014	0.1628

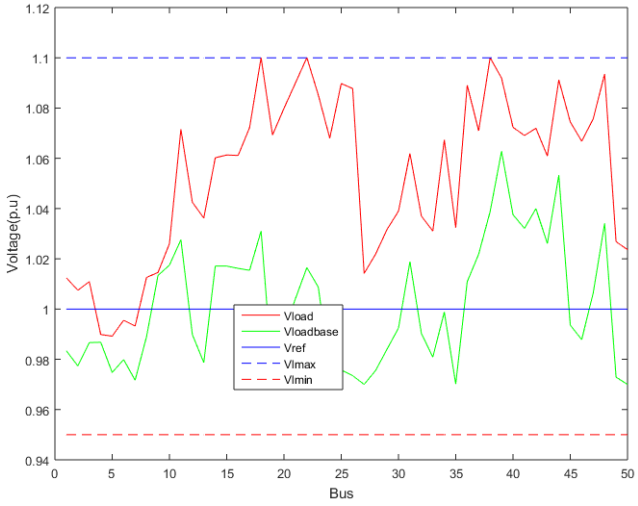

Fig. 12: Load voltage profile of IEEE 57-bus system when using Improved MFO Method

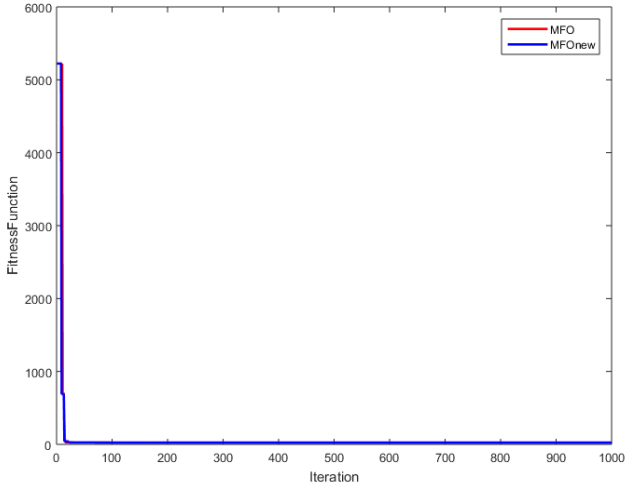

Fig. 13: Convergence characteristics of the compared methods in 57-bus system.

6.3 Case study 3

To evaluate the proposed method on large-scale systems, the improved MFO algorithm runs well on the huge IEEE 118-bus system. The evaluated testbed has 54 generators, 186 transmission lines, 64 load buses, and 9 transformers

with tap changers. We put 14 reactive power sources in the system. Table A.4 in the Appendix gives the placement and capacity of the VAR compensators.

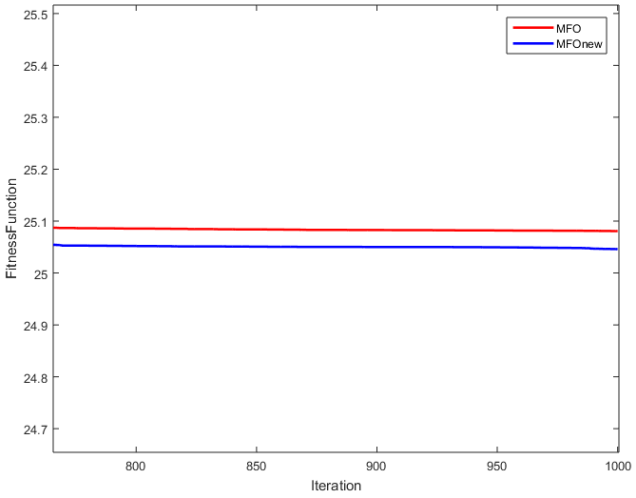

Fig. 14: Zoomed image of convergences at the end of search process in 57-bus system.

The analytical results two methods are presented in Tab. 3. All parameters of the improved MFO method are clearly superior to the conventional MFO Method. Comparing with other versions of the PSO and Gravitational Search Algorithm (GSA), the IMFO also gives the better solution. Once again, the proposed optimal solution accomplishes voltage constraints as Fig. 15. The convergence results of the two methods are presented in Fig. 16 and Fig. 17. In this benchmark, the conventional MFO converges faster than the proposed method. Nonetheless, at the end of the search progress, the proposed Improved MFO reaches the global solution. The detailed optimal solution of this case study is shown in Tab. A.9 in the Appendix.

Table 3: Analytical results of MFO and Improved MFO for the IEEE 118-bus system

Method	Best	Mean	SD
GSA [7]	127.76	-	-
PSO [15]	131.99	-	-
CLPSO [15]	130.96	-	-
OGSA [22]	126.99	-	-
MFO	125.8587	128.6239	1.9034
IMFO	124.9741	127.1519	1.4076

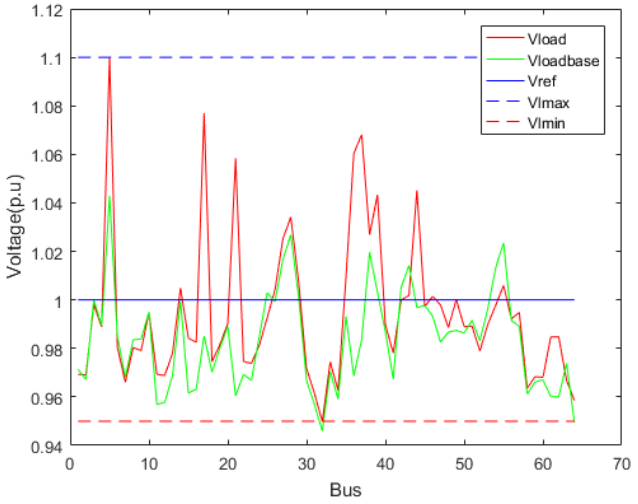

Fig. 15: Load voltage profile of IEEE 118-bus system when using Improved MFO Method.

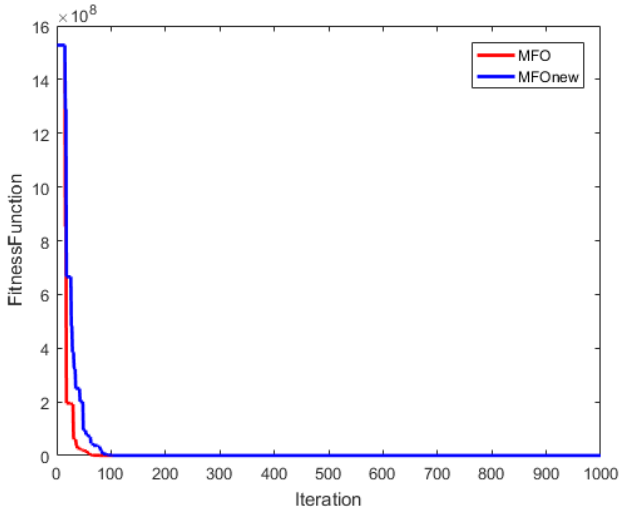

Fig. 16: Convergence characteristics of the compared methods in 118-bus system.

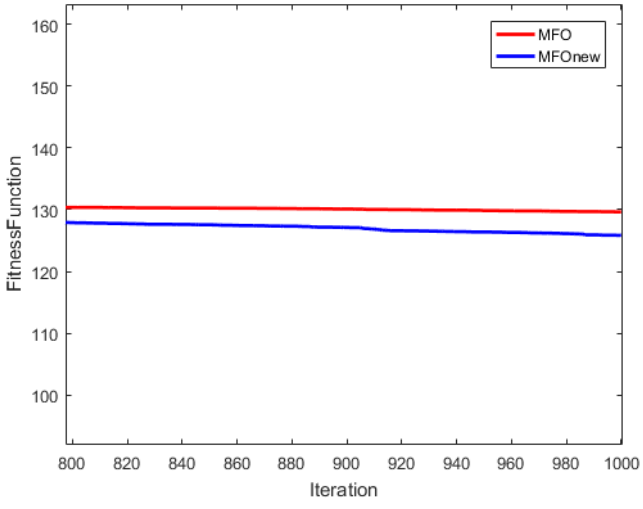

Fig. 17: Zoomed image of convergences at the end of search process in 118-bus system.

6.4 Case study 4

The last benchmark is an extremely complex IEEE 300-bus system. Only some algorithms successfully run on this grid. In that MFO algorithm is a powerful algorithm and can run on this grid with a high probability of convergence. Placement of capacitors is specified as in Tab. A.5 in the Appendix.

The best solution of two methods is presented in Tab. 4. The optimal solution satisfies all voltage constraints at 300 buses as Fig. 18.

Table 4: Analytical results of MFO and Improved MFO for IEEE 300-bus system

Method	Power losses [MW]
EGA [20]	646.2998
EEA [20]	650.6027
CSA [21]	635.8942
MFO	411.5256
IMFO	391.0417

Table 5: Comparison of statistics of MFO and Improved MFO for IEEE 300-bus system

Method	**MFO**	**Improved MFO**
Successful runs	3	10
Best	411.5256	391.0417
Mean	414.3143	401.6185
Worst	417.3142	409.203
SD	2.7479	6.7408

Table 6: Comparison of computation time of case studies

Method	Case study 1	Case study 2	Case study 3	Case study 4
IMFO	50s	66s	90s	172s
GSA [7]	198s	321s	1199s	-
GWO [24]	-	-	1372s	-
PSO [15]	-	-	1215s	-
CLPSO [15]	-	423s	1472s	-
OGSA [22]	190s	309s	1152s	-

Comparing the computational time, the proposed IMFO is robust algorithm. It takes only 90s to optimize the problem for the IEEE 118-bus system. On another hand, the IEEE 300-bus system is really a complex problem. The proposed IMFO only successfully gives the optimal solution in 10 of 50 runs, while the conventional MFO has only three times reached the optimal solution. The analytical statistics of the IEEE 300-bus system of the MFO and IMFO are shown in Tab. 5.

In Table 6, the computational times have been compared together. The proposed Improved MFO is a robust method while solving the problem only about few minutes. However, the methods have been run on different computer systems give the different computational times.

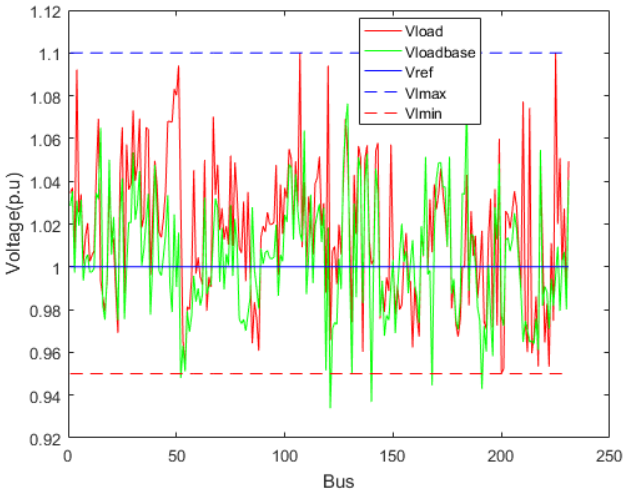

Figure 18: Load voltage profile of IEEE 300-bus system when using Improved MFO Method.

7. CONCLUSION

The proposed Improved MFO method is totally powerful and effective for minimizing the power loss in the grids. According to four benchmark systems, the proposed method has been shown to be more effective than conventional MFO and can solve relatively complex technical problems in electrical systems. Through the new method of limiting the number of flames, exploiting the optimal solution at the end of the loops makes the local solutions more accurate and helps the results of the problem converge to better values.

In future, the Improved MFO should be continued to enhance the performance of solutions.

ACKNOWLEDGEMENT

This research is funded by Vietnam National University HoChiMinh City (VNU-HCM) under grant number C2019-20-16.

REFERENCES

[1] Abou El Ela, AA., Abido, MA., and Spea, SR. 2011. Differential evolution algorithm for optimal reactive power dispatch. *Electric Power Systems Research*, 81(2):458–464.

[2] Alsac, O. and Stott, B. 1974. Optimal load flow with steady-state security. *IEEE transactions on power apparatus and systems*, (3):745–751.

[3] Aoki, K., Fan, M., and Nishikori, A. 1988. Optimal var planning by approximation method for recursive mixed-

integer linear programming. *IEEE Transactions on power Systems*, 3(4):1741–1747.

[4] Kürşat Ayan and Ulaş Kılıç. 2012. Artificial bee colony algorithm solution for optimal reactive power flow. *Applied soft computing*, 12(5):1477–1482.

[5] Erik Cuevas, Alonso Echavarría, and Marte A Ramírez-Ortegón. 2014. An optimization algorithm inspired by the states of matter that improves the balance between exploration and exploitation. *Applied intelligence*, 40(2):256–272.

[6] VA De Sousa, Edméa Cássia Baptista, and GRM Da Costa. 2012. Optimal reactive power flow via the modified barrier lagrangian function approach. *Electric Power Systems Research*, 84(1):159–164.

[7] Serhat Duman, Y Sönmez, U Güvenç, and N Yörükeren. 2012. Optimal reactive power dispatch using a gravitational search algorithm. *IET generation, transmission & distribution*, 6(6):563–576.

[8] Durairaj, S., Devaraj, D., and Kannan, PS. 2006. Genetic algorithm applications to optimal reactive power dispatch with voltage stability enhancement. *Journal-Institution of Engineers India Part El Electrical Engineering Division*, 87:42.

[9] Mohamed Abd El Aziz, Ahmed A Ewees, and Aboul Ella Hassanien. Whale optimization algorithm and moth-flame optimization for multilevel thresholding image segmentation. *Expert Systems with Applications*, 83:242–256, 2017.

[10] Mojtaba Ghasemi, Sahand Ghavidel, Mohammad Mehdi Ghanbarian, and Amir Habibi. 2014. A new hybrid algorithm for optimal reactive power dispatch problem with discrete and continuous control variables. *Applied soft computing*, 22:126–140.

[11] John Henry Holland et al. 1992. *Adaptation in natural and artificial systems: an introductory analysis with applications to biology, control, and artificial intelligence*. MIT press.

[12] Antony W Iorio and Xiaodong Li. 2006. Rotated test problems for assessing the performance of multi-objective optimization algorithms. In *Proceedings of the 8th annual conference on Genetic and evolutionary computation*, pages 683–690. ACM.

[13] Dung Ann Le and Dieu Ngoc Vo. 2012. Optimal reactive power dispatch by pseudo-gradient guided particle swarm optimization. In *2012 10th International Power & Energy Conference (IPEC)*, pages 7–12. IEEE.

[14] Zhiming Li, Yongquan Zhou, Sen Zhang, and Junmin Song. 2016. Lévy-flight moth-flame algorithm for function optimization and engineering design problems. *Mathematical Problems in Engineering*, 2016.

[15] Mahadevan, K. and Kannan, PS. 2010. Comprehensive learning particle swarm optimization for reactive power dispatch. *Applied soft computing*, 10(2):641–652.

[16] Seyedali Mirjalili. 2015. Moth-flame optimization algorithm: A novel nature-inspired heuristic paradigm. *Knowledge-Based Systems*, 89:228–249.

[17] Kenneth Price, Rainer M Storn, and Jouni A Lampinen. 2006. *Differential evolution: a practical approach to global optimization*. Springer Science & Business Media.

[18] Quintana, VH. and Santos-Nieto, M. 1989. Reactive-power dispatch by successive quadratic programming. *IEEE Transactions on Energy Conversion*, 4(3):425–435.

[19] Ingo Rechenberg. 1973. Evolution strategy: Optimization of technical systems by means of biological evolution. *Fromman-Holzboog, Stuttgart*, 104:15–16.

[20] Surender Reddy S., Bijwe, PR., and Abhyankar, AR. 2014. Faster evolutionary algorithm based optimal power flow using incremental variables. *International journal of electrical power & energy systems*, 54:198–210.

[21] Surender Reddy Salkuti. Optimal reactive power scheduling using cuckoo search algorithm. 2017. *International Journal of Electrical and Computer Engineering*, 7(5):2349.

[22] Binod Shaw, Vivekananda Mukherjee, and SP Ghoshal. 2014. Solution of reactive power dispatch of power systems by an opposition-based gravitational search algorithm. *International Journal of Electrical Power & Energy Systems*, 55:29–40.

[23] Yuhui Shi and Russell C Eberhart. 2001. Fuzzy adaptive particle swarm optimization. In *Proceedings of the 2001 congress on evolutionary computation (IEEE Cat. No. 01TH8546)*, volume 1, pages 101–106. IEEE.

[24] Mohd Herwan Sulaiman, Zuriani Mustaffa, Hamdan Daniyal, Mohd Rusllim Mohamed, and Omar Aliman. 2015. Solving optimal reactive power planning problem utilizing nature inspired computing techniques. *ARPN J. of Eng. and Appl. Sci*, 10(21).

[25] Mohd Herwan Sulaiman, Zuriani Mustaffa, Mohd Rusllim Mohamed, and Omar Aliman. 2015. Using the gray wolf optimizer for solving optimal reactive power dispatch problem. *Applied Soft Computing*, 32:286–292.

[26] Xin-She Yang. A new metaheuristic bat-inspired algorithm. 2010. In *Nature inspired cooperative strategies for optimization (NICSO 2010)*, pages 65–74. Springer.

[27] Xin-She Yang. 2012. Flower pollination algorithm for global optimization. In *International conference on unconventional computing and natural computation*, pages 240–249. Springer.

[28] Betül Sultan Yıldız and Ali Rıza Yıldız. 2017. Moth-flame optimization algorithm to determine optimal machining parameters in manufacturing processes. *Materials Testing*, 59(5):425–429.

[29] Ray Daniel Zimmerman, Carlos Edmundo Murillo-Sánchez, and Robert John Thomas. 2010. Matpower: Steady-state operations, planning, and analysis tools for power systems research and education. *IEEE Transactions on power systems*, 26(1):12-19.

APPENDIX

Table A.1: Outcomes of the unimodal tested functions

Function	Improved MFO		MFO		PSO		GSA	
F	Average	Standard deviation	Average	Standard deviation	Average	Standard deviation	Average	Standard deviation
F1	**1.08E-38**	4.42E-38	0.000117	1.321152	0.00015	1.153887	608.2328	464.6545
F2	**1.67E-23**	5.36E-23	0.000639	0.000877	7.715564	4.132128	22.75268	3.365135
F3	**133.3333**	938.0353	696.7309	188.5279	736.3931	361.7818	135760.8	48652.63
F4	**3.03E-02**	0.153942	70.68646	5.275051	12.97281	2.634432	78.78198	2.814108
F5	123.4518	517.9948	139.1487	**120.2607**	77360.83	77360.83	741.003	781.2393
F6	**1.79E-32**	3.24E-32	781.2393	9.87E-05	286.6518	107.0796	3080.964	898.6345
F7	**5.13E-03**	0.004628	0.091155	0.04642	1.037316	0.310315	0.112975	0.037607
Function	GA		FA		SMS		FPA	
F	Average	Standard deviation	Average	Standard deviation	Average	Standard deviation	Average	Standard deviation
F1	21886.03	2879.58	7480.746	894.8491	120	0	203.6389	78.39843
F2	56.51757	5.660857	39.3253	2.465865	0.020531	0.004718	11.1687	2.919591
F3	37010.29	5572.212	17357.32	1740.111	37820	0	237.5681	136.6463
F4	59.14331	4.648526	33.95356	1.86966	69.17001	3.876667	12.57284	2.29
F5	31321418	5264496	3795009	3795009	6382246	729967	10974.95	12057.29
F6	20964.83	3868.109	7828.726	975.2106	41439.39	3295.23	175.3808	63.45257
F7	13.37504	3.08149	1.906313	0.460056	0.04952	0.024015	0.135944	0.061212

Table A.2: Outcomes of the multimodal tested functions

Function	Improved MFO		MFO		PSO		GSA	
F	Average	Standard deviation	Average	Standard deviation	Average	Standard deviation	Average	Standard deviation
F8	-3.22E+03	3.57E+02	-8496.78	725.8737	-3571	430.7989	-2352.32	382.167
F9	2.06E+01	12.34089	84.60009	16.16658	124.2973	14.25096	31.00014	31.00014
F10	6.62E-01	3.33E+00	1.260383	1.26E+00	0.72956	1.568982	1.568982	3.740988
F11	0.158961	0.092246	0.01908	0.01908	0.021732	12.41865	12.41865	0.486826
F12	2.24E-01	0.471006	0.894006	0.88127	13.87378	5.85373	0.4634	0.137598
F13	2.97E-03	0.004902	0.115824	0.193042	11813.5	30701.9	7.617114	1.22532
Function	GA		FA		SMS		FPA	
F	Average	Standard deviation	Average	Standard deviation	Average	Standard deviation	Average	Standard deviation
F8	-6331.19	332.5668	-3662.05	214.1636	-3942.82	404.1603	-8086.74	155.3466
F9	236.8264	19.03359	214.8951	17.21912	152.8442	18.55352	92.69172	14.22398
F10	0.46751	0.531147	14.56769	0.46751	19.13259	0.238525	6.844839	1.249984
F11	179.9046	32.43956	69.65755	69.65755	420.5251	25.2561	2.716079	2.716079
F12	34131682	1893429	368400.8	172132.9	8742814	1405679	4.105339	1.043492
F13	1.08E+08	3849748	5557661	1689995	94.84298	0	62.3985	94.84298

Table A.3: Outcomes of the composite tested functions

Function	Improved MFO		MFO		PSO		GSA	
F	Average	Standard deviation	Average	Standard deviation	Average	Standard deviation	Average	Standard deviation
F14	2.35E+00	2.003747	8.25E-31	1.08E-30	137.7789	116.3128	5.43E-19	1.35E-19
F15	1.39E-03	0.002757	66.73272	53.22555	166.6643	164.3894	20.35852	63.12427
F16	-1.03E+00	1.56E-15	119.0146	28.3318	394.507	121.949	245.3021	49.05264
F17	3.98E-01	4.46E-16	345.4688	43.11578	486.3534	67.31685	315.2086	100.7477
F18	3.00E+00	0	10.4086	3.747669	256.5258	200.3816	70	48.30459
F19	-3.86E+00	0.00079	706.9953	194.9068	790.1284	189.4915	881.6392	45.17728
Function	GA		FA		SMS		FPA	
F	Average	Standard deviation	Average	Standard deviation	Average	Standard deviation	Average	Standard deviation
F14	92.13909	27.90131	175.9715	86.928	105.7572	26.8788	10.09454	31.59138
F15	96.7092	9.703147	353.6269	103.423	156.463	68.24926	11.41158	3.380957
F16	369.1036	42.84275	308.0516	37.435	406.9962	65.39732	234.9341	39.60663
F17	450.829	31.54446	548.5276	162.8993	518.6931	42.74199	355.3807	20.61705
F18	95.92017	53.79146	175.1975	83.15078	153.6984	96.91419	54.78722	42.05824
F19	523.7037	22.92001	829.5929	157.2787	611.5401	154.8529	573.0955	149.1538

Table A.4: Constraints of reactive generating devices in IEEE 118-bus system

Bus	5	34	37	44	45	46	48	74	79	82	83	105	107	110
$Q_{Ci,max}$ [MVar]	30	30	30	30	30	30	30	30	30	30	30	30	30	30
$Q_{Ci,min}$[MVar]	-10	-10	-10	-10	-10	-10	-10	-10	-10	-10	-10	-10	-10	-10

Table A.5: Constraints of reactive generating devices in IEEE 300-bus system

Bus	5	17	51	53	63	97	117	149	150	202	206	207	293
$Q_{Ci,max}[Mavr]$	30	30	30	30	30	30	30	30	30	30	30	30	30
$Q_{Ci,min}[Mavr]$	-10	-10	-10	-10	-10	-10	-10	-10	-10	-10	-10	-10	-10

Table A.6: Optimal solution given by the Improved MFO for the IEEE 118-bus system

V_{G1}	0.962	V_{G62}	1.015	V_{G113}	0.984	V_{G49}	1.032
V_{G4}	1.0	V_{G116}	1.025	V_{G65}	1.009	V_{G54}	0.958
V_{G6}	0.99	V_{G66}	1.053	Q_{C5}	30	V_{G55}	0.953
V_{G8}	1.053	V_{G69}	1.033	Q_{C34}	-14.683	V_{G56}	0.956
V_{G10}	1.1	V_{G70}	0.984	Q_{C37}	12.436	V_{G59}	0.985
V_{G12}	0.984	V_{G72}	0.986	Q_{C44}	4.485	V_{G61}	1.015
V_{G15}	0.972	V_{G73}	0.988	Q_{C45}	30	V_{G104}	0.976
V_{G18}	0.975	V_{G74}	0.962	Q_{C46}	-30	V_{G105}	0.97

V_{G19}	0.971	V_{G76}	0.95	Q_{C48}	6.211	V_{G107}	0.95
V_{G24}	0.997	V_{G77}	1.009	Q_{C74}	7.38	V_{G110}	0.974
V_{G25}	1.032	V_{G80}	1.03	Q_{C79}	30	V_{G111}	0.986
V_{G26}	1.099	V_{G85}	1.007	Q_{C82}	29.438	V_{G112}	0.968
V_{G27}	0.977	V_{G87}	1.011	Q_{C83}	21.258	T_{63-59}	1.019
V_{G31}	0.968	V_{G89}	1.026	Q_{C105}	29.999	T_{64-61}	1.016
V_{G32}	0.973	V_{G90}	0.999	Q_{C107}	15.187	T_{65-66}	0.94
V_{G34}	0.99	V_{G91}	0.996	Q_{C110}	23.159	T_{68-69}	0.936
V_{G36}	0.987	V_{G92}	1.006	T_{8-5}	1.049	T_{81-80}	0.964
V_{G40}	0.976	V_{G99}	1.007	T_{26-25}	1.1		
V_{G42}	0.987	V_{G100}	1.011	T_{30-17}	1.062		
V_{G46}	1.015	V_{G103}	0.997	T_{38-37}	1.036		